

Crystal Structures and Conformational Analysis of Complexes of the Type $\text{Cp}_2\text{Ti}(\text{SiHRR}')\text{PMe}_3$ ($\text{R}, \text{R}' = \text{H}, \text{Me}, \text{Ph}$): Relationships between Calculated Molecular Structures and Observed Solid-State Structures

James Britten, Ying Mu, and John F. Harrod

Chemistry Department, McGill University, Montreal, Quebec, Canada H3A 2K6

Joel Polowin and Michael C. Baird*

Chemistry Department, Queens University, Kingston, Ontario, Canada K7L 3N6

Edmond Samuel

Laboratoire de Chimie Organométallique de l'ENSCP (URA 403 CNRS),
11 rue P. et M. Curie, 75005 Paris, France

Received October 13, 1993

In an effort to understand the effects of steric factors on catalytic silane dehydrocoupling reactions, the X-ray crystal structures of the catalyst model compounds $\text{Cp}_2\text{Ti}(\text{SiH}_2\text{Ph})\text{PMe}_3$ [$a = 8.548(2)$ Å, $b = 9.098(2)$ Å, $c = 12.786(2)$ Å, $\beta = 101.48(2)^\circ$; monoclinic, $P2_1$; 2 molecules per unit cell] and $\text{Cp}_2\text{Ti}(\text{SiHMePh})\text{PMe}_3$ [$a = 9.076(3)$ Å, $b = 12.078(4)$ Å, $c = 18.299(5)$; orthorhombic, $P2_12_12_1$; 4 molecules per unit cell] were determined and compared to those of similar compounds from the literature. The conformational energy profiles for silyl ligand rotation in these two compounds and in $\text{Cp}_2\text{Ti}(\text{SiHPh}_2)\text{PMe}_3$, obtained utilizing molecular mechanics calculations, suggest that the conformations, and apparently distorted Ti-Si-C(ipso) angles, exhibited in the solid state by all three compounds are determined by intramolecular steric factors.

Introduction

Metalocene derivatives of the group 4 elements exhibit remarkable activity as catalysts for the dehydrocoupling of primary organosilanes¹⁻⁵ and germanes.⁶ Combined with this high activity is a marked sensitivity to steric factors, which appear to play a major role in determining the selectivity toward primary, as opposed to secondary and tertiary, silanes and in determining selectivity toward linear chain propagation as opposed to cyclization.^{1d,2c,7,8}

The most favored mechanistic proposal to explain the complex reactions observed in these systems is the σ -bond

(1) (a) Aitken, C. T.; Harrod, J. F.; Samuel, E. J. *Am. Chem. Soc.* 1986, 108, 4059. (b) Aitken, C.; Harrod, J. F.; Samuel, E. *Can. J. Chem.* 1986, 64, 1677. (c) Aitken, C.; Barry, J.-P.; Gauvin, F.; Harrod, J. F.; Malek, A.; Rousseau, D. *Organometallics* 1989, 8, 1732. (d) Gauvin, F.; Harrod, J. F. *Can. J. Chem.* 1990, 68, 1638. (e) Mu, Y.; Aitken, C.; Côté, B.; Harrod, J. F.; Samuel, E. *Can. J. Chem.* 1991, 69, 264.

(2) (a) Woo, H. G.; Tilley, T. D. *J. Am. Chem. Soc.* 1989, 111, 8043. (b) Woo, H. G.; Tilley, T. D. *J. Am. Chem. Soc.* 1989, 111, 3757. (c) Tilley, T. D. *Comments Inorg. Chem.* 1990, 10, 37. (d) Woo, H. G.; Tilley, T. D. In *Inorganic and Organometallic Oligomers and Polymers*; Laine, R. M.; Harrod, J. F., Eds.; Kluwer Publishers, Amsterdam, 1991, p 3. (e) Tilley, T. D. *Acc. Chem. Res.* 1993, 26, 22.

(3) (a) Corey, J. Y.; Chang, L. S.; Corey, E. R. *Organometallics* 1987, 6, 1595. (b) Chang, L. S.; Corey, J. Y. *Organometallics* 1989, 8, 1885. (c) Corey, J. Y.; Zhu, X.-H.; Bedard, T. C.; Lange, L. D. *Organometallics* 1991, 10, 924. (d) Corey, J. Y.; Zhu, X.-H. *Organometallics* 1992, 11, 672.

(4) Campbell, W. H.; Hilty, T. K.; Yurga, L. *Organometallics* 1989, 8, 2615.

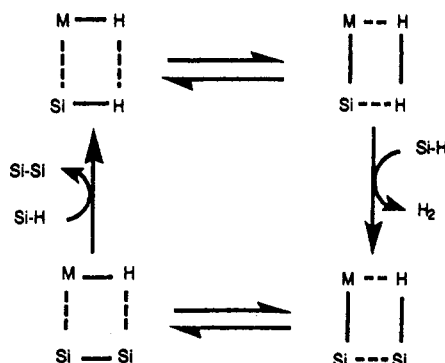
(5) Banovetz, J. P.; Stein, K. M.; Waymouth, R. M. *Organometallics* 1991, 10, 3430.

(6) Aitken, C.; Harrod, J. F.; Malek, A.; Samuel, E. *J. Organomet. Chem.* 1988, 349, 285.

(7) Harrod, J. F. In *Transformation of Organometallics into Common and Exotic Materials: Design, and Activation*; R. M. Laine, Ed.; Martinus Nijhoff, Amsterdam, 1988, p 103.

(8) Woo, H. G.; Waltzer, J. F.; Tilley, T. D. *J. Am. Chem. Soc.* 1992, 114, 7047.

Scheme I. The Four-Center Transition States Involved in the σ -Bond Metathesis Mechanism



metathesis mechanism of Woo and Tilley,² the essential features of which are summarized in Scheme I. The reactions of this scheme involve the formation and cleavage of Si-Si bonds, the cleavage and formation of Si-H bonds, and the cleavage and formation of H-H bonds. Tilley has qualitatively concluded,⁸ on the basis of steric arguments, that the energies of the relevant, bimolecular, 4-center transition states will be in the order $\text{M-H}\cdots\text{RSiH}_3 < \text{M-H}\cdots\text{RH}_2\text{Si}(\text{SiHR})_n\text{SiH}_2\text{R} < \text{M}-(\text{SiHR})_n\text{SiH}_2\text{R}\cdots\text{RSiH}_3 < \text{M}-(\text{SiHR})_n\text{SiH}_2\text{R}\cdots\text{RH}_2\text{Si}(\text{SiHR})_n\text{SiH}_2\text{R}$. By similar reasoning, it was concluded that cyclization is more likely to occur through the less congested transition state involving intramolecular closure of $\text{M-Si}\cdots\text{SiH}_2\text{R}$, rather than by back-biting, which would require the more congested $\text{M-Si}\cdots\text{SiH}(\text{R})\cdots\text{SiH}_2\text{R}$ transition state.

Possibly relevant to the issue of steric effects, we have previously reported that the crystal structures of the compounds $\text{Cp}_2\text{Ti}(\text{SiHPh}_2)\text{PMe}_3$ (1: Cp = η^5 -cyclopent-

Table I. Crystal Data and Data Collection Parameters for Compounds 2 and 3

	2	3
formula	$C_{19}H_{26}PSiTi$	$C_{20}H_{28}PSiTi$
fw	361.37	375.40
system	monoclinic	orthorhombic
space group	$P2_1$	$P2_12_12_1$
<i>a</i> , Å	8.548(2)	9.076(3)
<i>b</i> , Å	9.098(2)	12.078(4)
<i>c</i> , Å	12.786(2)	18.299(5)
β , deg	101.48(2)	
$\alpha = \beta = \gamma$, deg		90
<i>V</i> , Å ³	974(1)	2006(1)
<i>Z</i>	2	4
<i>F</i> (000)	382	796
ρ (calcd), kg/L	1.23	1.243
μ (Mo K α), cm ⁻¹	5.9	5.562
cryst dimens, mm	0.2 × 0.3 × 0.5	0.4 × 0.4 × 0.4
temp, °C	20	20
radiation (graphite monochromator)	Mo K α ($\lambda = 0.710 69$ Å)	Mo K α ($\lambda = 0.710 69$ Å)
2 θ limits, deg	3 < 2 θ < 60	3 < 2 θ < 55
scan speed, deg/min	7	6
no. of total rflns	3258	2624
no. of reflns used	2077	1440
variables	215	208
<i>R</i>	0.038	0.052
<i>R</i> _w	0.041	0.03

tadienyl, Me = methyl) and $Cp_2Ti(SiH_2Ph)PEt_3$ (Et = ethyl) both assume conformations in which a phenyl group is essentially gauche to the two Cp groups, i.e. folded back away from the trialkylphosphine group and toward the Cp_2Ti moiety. In addition, for this phenyl group, both compounds also display rather large Ti–Si–C(ipsos) bond angles (116.8(1)° and 114.4(5)°, respectively)⁹, presumably because of steric repulsions from the Cp groups. Interestingly, the Ti–Si–C(ipsos) bond angle of the second phenyl group of 1, which is gauche to both a Cp group and the apparently more sterically demanding PMe_3 ligand, is 121.3(1)°. Since these compounds are believed to be structurally related to catalytic intermediates, it is of interest to determine whether the apparent distortions are a coincidental result of crystal packing forces or if they result from some intrinsic molecular property, steric or electronic. In an attempt to deal with this question, we have therefore extended the number of compounds of this type for which crystallographic data are available by determining the crystal structures of the compounds $Cp_2Ti(SiH_2Ph)PMe_3$ (2) and $Cp_2Ti(SiHMePh)PMe_3$ (3). Complementing the crystallographic investigation, we have also carried out on compounds 1–3 extensive molecular mechanics (MM) calculations in which we have investigated the conformational energy profiles for silyl ligand rotation. The results of this study and their relevance to the mechanism of the catalytic process are the subject of the present paper.

Results and Discussion

Structures of Compounds 2 and 3. The resolution of the structure of compound 2 presented no problems and the molecular parameters are essentially identical to those of the analogous triethylphosphine complex reported previously.⁹ The resolution of the structure of 3 presented some problems due to cocrystallization of the two enantiomers. This results in disordering between the Si–H and Si–Me groups, with a refined occupancy of 0.71:0.29. Despite this disorder, the model gives a satisfactory refinement and the general agreement of the bond

Table II. Atomic Coordinates and Isotropic Thermal Parameters for 2

atom	<i>x</i>	<i>y</i>	<i>z</i>	<i>U</i> _{eq} , Å ²
Ti	0.1107(1)	0.5000	0.2657(1)	0.037(1)
P	0.1653(1)	0.7791(1)	0.2748(1)	0.050(1)
Si	0.4203(1)	0.4958(2)	0.2647(1)	0.050(1)
C(1)	0.2256(7)	0.6691(6)	0.1624(4)	0.075(2)
C(2)	0.3159(7)	0.8481(6)	0.3846(4)	0.073(2)
C(3)	-0.0065(8)	0.8909(7)	0.2891(6)	0.105(3)
C(11)	0.2174(7)	0.4741(10)	0.4507(3)	0.094(3)
C(12)	0.0804(9)	0.5549(7)	0.4422(3)	0.092(3)
C(13)	-0.0452(7)	0.4678(9)	0.3978(4)	0.094(3)
C(14)	0.0129(8)	0.3345(8)	0.3801(4)	0.095(3)
C(15)	0.1760(8)	0.3379(7)	0.4119(4)	0.094(3)
C(21)	0.1029(5)	0.5052(8)	0.0806(3)	0.076(2)
C(22)	-0.0340(6)	0.5818(6)	0.0969(3)	0.067(2)
C(23)	-0.1284(5)	0.4831(7)	0.1367(3)	0.065(2)
C(24)	-0.0579(5)	0.3457(6)	0.1426(4)	0.066(2)
C(25)	0.0855(6)	0.3586(7)	0.1097(4)	0.073(2)
C(31)	0.5000(4)	0.3155(5)	0.2200(3)	0.048(1)
C(32)	0.4926(5)	0.2825(6)	0.1126(3)	0.056(1)
C(33)	0.5445(5)	0.1503(6)	0.0802(3)	0.064(2)
C(34)	0.6049(5)	0.0448(5)	0.1522(4)	0.063(2)
C(35)	0.6127(5)	0.0713(6)	0.2592(4)	0.065(2)
C(36)	0.5617(5)	0.2051(6)	0.2914(3)	0.059(1)

^a Equivalent isotropic *U* defined as one-third of the trace of the orthogonalized *U*_{ij} tensor.

Table III. Atomic Coordinates and Isotropic Thermal Parameters for 3

atom	<i>x</i>	<i>y</i>	<i>z</i>	<i>U</i> _{eq} , Å ²
Ti	0.1102(1)	1.0031(2)	0.5785(1)	0.030(1)
P	-0.1711(2)	0.9846(4)	0.5864(1)	0.045(1)
Si	0.1020(2)	0.9905(4)	0.7228(1)	0.049(1)
C(1)	0.206(3)	1.177(1)	0.609(1)	0.09(1)
C(2)	0.294(2)	1.138(1)	0.550(2)	0.11(1)
C(3)	0.181(2)	1.134(1)	0.492(1)	0.066(9)
C(4)	0.058(2)	1.166(1)	0.520(1)	0.065(9)
C(5)	0.063(3)	1.196(1)	0.588(1)	0.09(1)
C(6)	0.059(2)	0.814(1)	0.544(2)	0.09(1)
C(7)	0.138(3)	0.863(2)	0.487(1)	0.09(1)
C(8)	0.276(2)	0.894(1)	0.513(1)	0.07(1)
C(9)	0.281(2)	0.858(1)	0.581(1)	0.067(9)
C(10)	0.158(2)	0.813(1)	0.604(1)	0.058(8)
C(11)	-0.272(1)	1.099(1)	0.629(1)	0.09(1)
C(12)	-0.247(1)	0.869(1)	0.636(1)	0.09(1)
C(13)	-0.262(1)	0.969(2)	0.4975(4)	0.10(1)
C(14)	0.375(2)	1.075(2)	0.7800(9)	0.08(1)
C(15)	0.526(2)	1.070(1)	0.8068(8)	0.08(1)
C(16)	0.570(2)	0.965(2)	0.8174(9)	0.09(1)
C(17)	0.499(2)	0.866(1)	0.8020(9)	0.09(1)
C(18)	0.358(2)	0.882(1)	0.7762(9)	0.08(1)
C(19)	0.294(1)	0.988(2)	0.7635(4)	0.059(6)
C(20)	0.012(2)	1.099(1)	0.7785(8)	0.055(3)
C(21)	-0.012(4)	0.934(3)	0.789(2)	0.055

^a Equivalent isotropic *U* defined as one-third of the trace of the orthogonalized *U*_{ij} tensor.

parameters with the other structures lends confidence that it is correct. The crystal and data collection parameters for 2 and 3 are listed in Table I, positional parameters in Tables II and III. Important molecular parameters for 2 and 3, and, for comparison, 1 and $Cp_2Ti(SiH_2Ph)PEt_3$, are given in Table IV, together with the calculated values for comparison. ORTEP drawings of the structures of 2 and 3, with the atom numbering schemes, are given in Figures 1 and 2.

As can be seen, the bond lengths and angles of 2 and 3 are generally comparable with those previously established for 1 and $Cp_2Ti(SiH_2Ph)PEt_3$. The most significant features of the structures of 2 and 3 are that the phenyl groups again assume positions gauche to the two Cp ligands, with the Ti–Si–C(ipsos) angles being 115.5(1)° and 111.6(2)°, respectively. In addition, the Ti–Si–Me angles of the two enantiomers of 3 are 121.4(5)° and 138(1)°,

(9) Samuel, E.; Mu, Y.; Harrod, J. F.; Dromzee, Y.; Jeannin, Y. *J. Am. Chem. Soc.* 1990, 112, 3435.

Table IV. Comparison of Crystallographic and MM Values for Selected Bond Lengths (Å) and Angles (deg) for Compounds 1–3

parameter	1		2		3	
	MM	X-ray	MM	X-ray	MM	X-ray
Ti–Si	2.488	2.652(1)	2.485	2.650(1)	2.487(S); 2.488(R)	2.646(2)
Ti–P	2.608	2.609(1)	2.498	2.580(1)	2.499; 2.496	2.567(2)
Ti–Cp(1)	2.263	2.054(2)	2.255	2.065(5)	2.246; 2.290	2.03(1)
Ti–Cp(2)	2.299	2.058(2)	2.251	2.048(4)	2.276; 2.268	2.07(1)
P–Ti–Si	96.57	84.8(1)	89.04	80.9(1)	94.42; 97.36	80.9(1)
P–Ti–Cp(1)	105.28	107.6(2)	108.36	107.1(2)	107.13; 108.85	108.5(5)
P–Ti–Cp(2)	107.51	106.5(1)	108.04	106.9(2)	107.78; 106.52	104.1(4)
Ti–Si–Ph(1)	114.55	116.8(1)	114.88	115.5(1)	113.38; 112.94	111.6(2)
Ti–Si–Ph(2)	114.55	121.3(1)				
Ti–Si–Me					112.9; 113.2	121.4(5); 138(1)

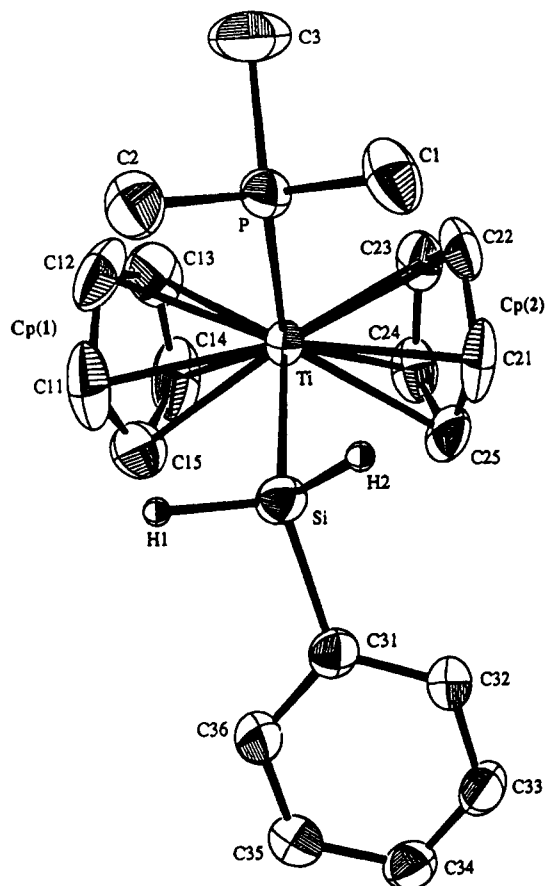


Figure 1. An ORTEP diagram of compound 2 showing the atom numbering scheme.

particularly large and suggestive of considerable steric interaction with neighboring Cp and PMe_3 ligands. It is possible that the large difference between these two experimental parameters is related to the disorder problem. Despite the wide variation in the steric demands of the silyl ligands, the Cp–Ti–Cp angles for all four compounds remain constant at $135.6(4)^\circ$.

Conformational Analysis of 1–3. We have previously shown that MMX calculations on a variety of η^5 -cyclopentadienyliron^{10b} and arenechromium^{10c} compounds result in computed conformational energy profiles for alkyl, acyl, and tertiary phosphine ligand rotations which agree very well with the results of experimental studies. In particular, experimentally determined conformational energy differences as small as $1\text{--}3 \text{ kcal mol}^{-1}$ were successfully reproduced computationally, apparently lending credence to the MMX methodology.¹¹

(10) (a) Mackie, S. C.; Park, Y.-S.; Shurvell, H. F.; Baird, M. C. *Organometallics* 1991, 10, 2993. (b) Mackie, S. C.; Baird, M. C. *Organometallics*, 1992, 11, 3712. (c) Polowin, J. E.; Mackie, S. C.; Baird, M. C. *Organometallics* 1992, 11, 3724.

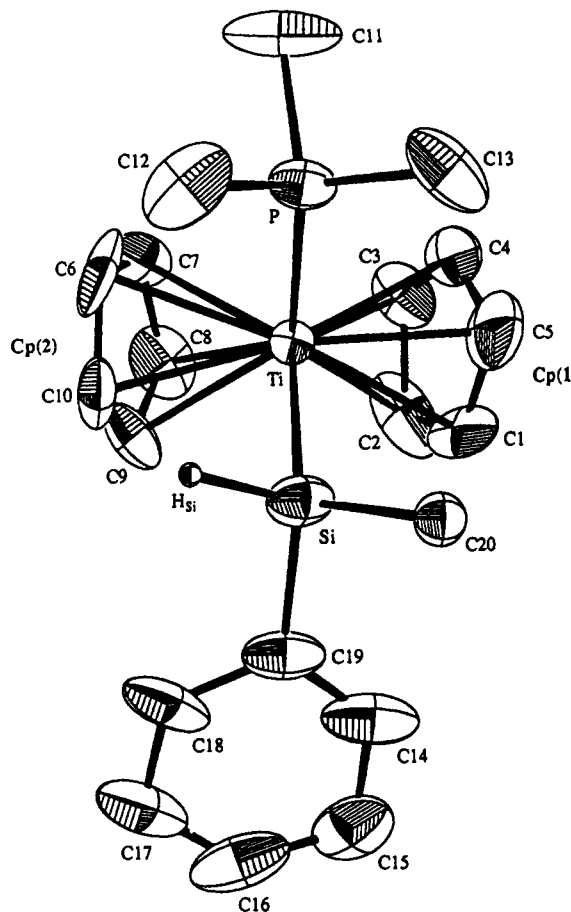


Figure 2. An ORTEP diagram of compound 3 showing the atom numbering scheme.

Optimization of the geometries of 1–3 as described in the Experimental Section resulted in structures similar to those established crystallographically for the compounds. The titanium–ligand bond distances and ligand–titanium–ligand bond angles are generally well within 0.2 \AA and 10° , respectively, of the corresponding crystallographic bond length and bond angle data. In particular, the Ti–Si–C(ipso) bond angles were calculated to be 114.0° and 114.6° (1), 114.9° (2), and 112.9° and 113.2° (two enantiomers of 3), in good agreement with the crystallographic data. These angles appear to be opened up because of steric factors, since similar calculations on the sterically unencumbered SiMePhH_2 yielded a very reasonable C–Si–C(ipso) bond angle of 109.5° . The agreement between the calculated Ti–Si– CH_3 angle (ca. 112°) and the crystallographic values (121° , major enantiomer, 138° , minor enantiomer) for 3 is much poorer. This is not unexpected since this angle

(11) Available as PCMODEL from Serena Software, Bloomington, IN. See: Gajewski, J. J.; Gilbert, K. E.; McKelvey, J. In *Advances in Molecular Modeling*; Liotta, D., Ed.; JAI Press: Greenwich, CT, 1990; Vol. 2, p 65.

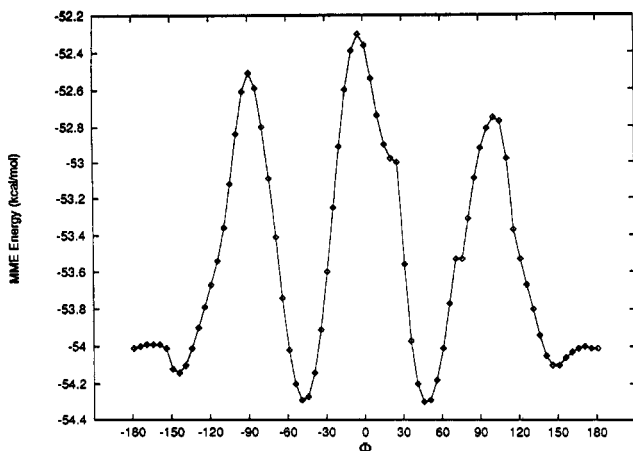
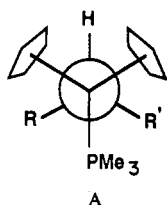


Figure 3. Variation of the conformational energy of **2** with the dihedral angle P-Ti-Si-C(ipsi).

is the one most affected by the disorder problem, while the MM calculations for **3** are of poorer quality than those for the other compounds (vide infra).

While the overall computational results are quite respectable, it was realized that the steep dependence of ligand-ligand van der Waals repulsions on distance could result in errors in estimations of the interligand steric interactions during operations of the dihedral driver. Calculations of conformational energy profiles were therefore carried out, as previously,¹⁰ with all metal-ligand distances set to crystallographic distances and "fixed" with very high stretching force constants of 50 mdy \AA^{-1} .

It is convenient to consider the titanium atoms in the complexes under consideration here to be topologically four-coordinate; thus various conformations may be conceived in which the ligands on the titanium and the substituents on the silicon atoms of the coordinated silyl groups are mutually staggered, as in the Newman projection of $Cp_2Ti(SiHRR')(PMe_3)$ (**A**).



For **2**, the dihedral angle driven was C(ipsi)-Si-Ti-P, such that the dihedral (torsional) angle (ϕ) = 0 when the Ph ring eclipses the P atom. The conformational energy of **2** as a function of ϕ is illustrated in Figure 3, which shows a doubly degenerate global minimum when the Ph group is situated between the PMe_3 and one of the Cp ligands ($\phi \approx \pm 45^\circ$) and a doubly degenerate local minimum when the Ph group lies between the two Cp groups ($\phi \approx \pm 145^\circ$); the latter do not coincide at precisely $\phi = 180^\circ$ because of tilting of the phenyl group. The energy differences between these two pairs of minima, ~ 0.2 kcal mol^{-1} are probably not significant, and we note that the observed value of ϕ in the crystal structure is 150° . The global energy maximum occurs when $\phi \approx 0^\circ$, at which the Ph group eclipses the PMe_3 , and local maxima occur when $\phi \approx -90^\circ$ and 115° , at which the Ph group interacts with the two Cp ligands. The energy differences, < 0.5 kcal mol^{-1} , may not be significant. The calculated barrier to rotation is ~ 1.6 kcal mol^{-1} .

The variations in the Si-Ti-Cp(centroid), the P-Ti-Si, and P-Ti-Cp(centroid) bond angles during silyl group rotation are essentially as expected on the basis of

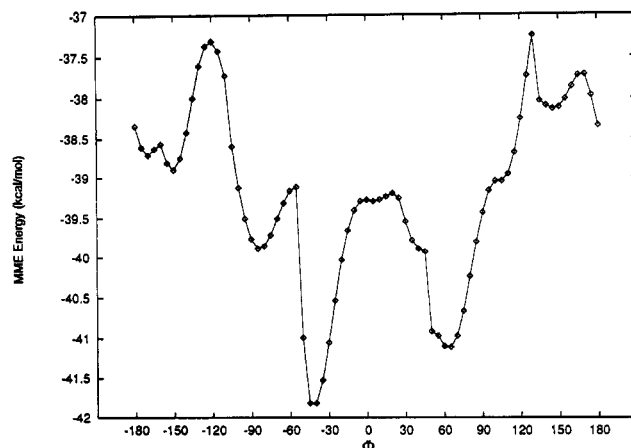


Figure 4. Variation of the conformational energy of **1** with the dihedral angle H-Si-Ti-P.

anticipated steric repulsions. The Si-Ti-Cp(centroid) bond angle is at a maximum when the Ph eclipses the Cp ligand in question, at which point the other Si-Ti-Cp(centroid) bond angle is at a minimum. The P-Ti-Si bond angle is at a maximum at $\phi = 0^\circ$, when the Ph group is close to the PMe_3 ligand, and at a minimum when it is 180° away, the position in which it interacts with the two Cp groups. The P-Ti-Cp(centroid) bond angles exhibit significant minima when the phenyl group lies between the Cp ligands, presumably because steric repulsions force the Cp ligands toward the PMe_3 ligand. On the other hand, the Ti-Si-C(ipsi) bond angle is large when the phenyl group eclipses the other ligands. Finally, rotation of the $PhSiH_2$ group does not induce rotation of the PMe_3 ; the lack of synchronization of these motions indicates the absence of a "gearing" effect.

For compound **1**, the dihedral (torsional) angle driven was H-Si-Ti-P, such that $\phi = 0^\circ$ when the H atom of the silyl group eclipses the P atom. The conformational energy plot of **1** is illustrated in Figure 4. The global minimum occurs at $\phi \approx -45^\circ$, when one of the Ph groups lies between the two Cp ligands and the other between a Cp ligand and the PMe_3 . A local minimum (by 0.7 kcal mol^{-1}), which corresponds approximately to the crystallographic structure, lies at $\phi \approx 60^\circ$. These two conformations, which appear in their Newman projections to be mirror images, and might therefore be isoenergetic, are rendered diastereomeric by the orientations of the phenyl groups.¹²

There is also a local minimum at $\phi \approx 150^\circ$, at which the H atom lies between the two Cp ligands, approximately degenerate global maxima at $\phi \approx \pm 120^\circ$, at which the Ph groups essentially eclipse a Cp and the PMe_3 , and a local maximum at $\phi \approx 0^\circ$, at which each Ph group eclipses a Cp ligand. The lack of a plane of symmetry in the conformational energy profile arises both because the angles at titanium and silicon are quite different and because of the abovementioned tilting of the phenyl rings, which results in unequal interactions of the phenyl rings with the ligands on the titanium.¹² The global barrier to rotation of the silyl group in **2** is 4.6 kcal/mol.

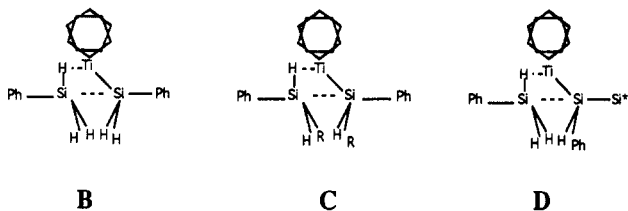
For compound **3**, the driven dihedral angle was the P-Ti-Si-C(ipsi) torsion, such that $\phi = 0^\circ$ when the ipso carbon atom of the phenyl group eclipses the P atom. The conformational energy plots for this compound were less regular than those of **1** and **2**, due to the complex topology of the $MePhHSi$ ligand and the chirality at the Si. At the

(12) For relevant discussions, see: ref 10c and Brunner, H.; Hammer, B.; Krüger, C.; Angermund, K.; Bernal, I. *Organometallics* 1985, 4, 1063.

level of computation to which we chose to limit our effort, the outputs were of lower quality than those reported for 1 and 2. Nevertheless, the conformational plots do exhibit the expected 3-fold rotational barriers, with global, or near-global, minima at $\phi \approx 180^\circ$. This is essentially the staggered conformation exhibited in the crystal structure, in which the Ph group lies between the two Cp ligands. The differences between minima are <1.5 kcal/mol. The global barrier to rotation of the silyl group is 5.3 kcal/mol.

The results of our calculations show a strong correlation with the structures obtained by X-ray crystallography. It therefore seems that the conformations adopted in the solid state by 1–3 are all close to the minimum molecular energy conformations, although bond and dihedral angle distortions arising from ligand rotation are clearly facile. It is also clear from the calculations that, although the overall barriers to rotation of the silyl ligands are quite small, the calculated differences between that of the primary silyl, PhSiH₂, and those of the secondary silyls, Ph₂SiH and PhMeSiH, 3.0–3.5 kcal/mol, are in the right range to account for the differences in rates of dehydrocoupling of these classes of silane (ca. 10²). Since there is no relatively sterically demanding phosphine in the actual catalytic system, however, it seems likely that the barriers to the silyl rotation necessary to achieve the transition state during the catalytic process are even lower than those calculated here. On the other hand, were the catalytic process to be a σ -bond metathesis at coordinately unsaturated Ti(III) center, then the complexes 1–3 could be interesting models.

The species B–D are three schematic transition states based on the above model, and on the proposal of Tilley



for the zirconocene(IV)-catalyzed reaction.^{2a} The state B corresponds to the formation of the first Si–Si bond, for which no stereochemically significant outcome is possible with a primary silane. The state C is the most likely conformation for the formation of a disilane from a secondary monosilane, such as PhMeSiH₂. A rotational barrier in this transition state comparable to that calculated for the compounds 2 and 3, i.e. ca. 3 kcal, should favor the racemic isomer by 1–2 orders of magnitude. Corey and co-workers reported a statistical distribution of the isomers of the trimer resulting from dehydrocoupling of MePhSiH₂, catalyzed by a zirconocene-based catalyst, but the tetrasilane appeared to give a nonstatistical distribution.^{3c} The isomeric compositions of oligomers produced with a titanocene-based catalyst were not reported. In view of the larger size of zirconium, relative to titanium, it is hard to assess the significance of this observation. The transition state D is that proposed for the chain elongation step, in the presence of unconsumed monosilane. It must be remembered that there will also be important steric contributions to the energies of these three transition states arising from the change in coordination of the free silane from four to five.

Experimental Section

Synthesis of 2 and 3. These compounds were prepared using the same conditions as those used for the synthesis of 1.⁹ 2 and

3 were both obtained directly as crystals suitable for X-ray analysis in 90% and 88% yields, respectively. Analysis for 2: Calcd for C₁₉H₂₆PSiTi: C, 63.15; H, 7.25. Found: C, 62.42; H, 6.78. EPR (–20 °C): doublet of triplets; a(P), 29.3G; a(H), 3.2G; a(Ti), 8.7G; g(iso), 1.9944. Analysis for 3: Calcd for C₂₀H₂₈PSiTi: C, 63.83; H, 7.45. Found: C, 62.58; H, 7.91. EPR(–20 °C): doublet of doublets; a(P), 29.0G; a(H), 2.9G; a(Ti), 8.3G; g(iso), 1.9966.

Crystal Structure Determinations. The data for compound 2 were collected and refined by Dr. Zhongsheng Jin of Laboratory 26, Changchung Institute for Applied Chemistry, Academia Sinica. The data were corrected for absorption, Lorentz, and polarization effects. A crystal was sealed under argon in a thin-walled capillary. Diffraction measurements were carried out on a Nicolet R3M/E diffractometer. Crystal data and data collection parameters are listed in Table I. Computations were performed using the SHELXTL¹³ system adapted to an Eclipse S/140 computer. The space group P2₁ was established by systematic absences in the complete dataset (0k0, $k = 2n + 1$). The positions of Ti atoms were deduced from the Patterson map. The positions of the P, Si, and C atoms were determined by difference Fourier syntheses and refined by full-matrix least squares and with anisotropic thermal parameters. The hydrogen atoms, other than those on Si, were calculated and fixed in their ideal positions. The two hydrogen atoms on Si were located on a differential Fourier map and the positions were refined by full-matrix least squares.

The data for the crystal structure determination of 3 were collected at Crystallitics Co. on a Syntex P21 diffractometer using Mo radiation. The structure was solved using SHELXS86 and refined in TEXSAN.¹⁴ No absorption correction was applied. The absolute configuration could not be determined. The non-hydrogen atoms were refined anisotropically. The hydrogens were fixed in calculated positions. The Me/H disorder on Si was refined with C(20) and C(21) having a common isotropic temperature factor and refined occupancy. Models involving phenyl group disorder did not refine satisfactorily.

Molecular Mechanics Calculations. The MM calculations were performed on a Sun SPARCStation 1 using MMX, the minimization routine within the commercial modeling program PCMODEL 4.0, from Serena Software.¹¹ Input and optimization procedures were carried out much as described previously;¹⁰ the Ti–Si bond parameters were $k = 2.00$ mdyn Å^{–1}, $L_0 = 2.27$ Å. The structures of 1–3 were read into PCMODEL in the X-ray format and the atom types, connectivities, etc. were edited as appropriate using a text editor.

The dihedral driver of PCMODEL was employed to compute the silyl ligand rotational conformational energy profiles of 1–3, metal–ligand bond distances being set to the crystallographic distances and fixed with very high stretching force constants of 50 mdyn Å^{–1}. The energy changes associated with bond rotations were computed using the dihedral driver within PCMODEL, and plots of energy versus torsional angle are used to illustrate the rotational energy profiles. In all cases, rotations were taken through $>360^\circ$, showing that the reproducibility of the calculated energies was generally within about 0.2 kcal mol^{–1}.

Acknowledgment. We thank the Natural Sciences and Engineering Research Council of Canada (M.C.B and J.F.H), the Fonds FCAR du Québec (J.F.H), and NATO (J.F.H and E.S) for the Research Grants that made this work possible, and the Government of Ontario for an Ontario Graduate Scholarship to J.E.P.

Supplementary Material Available: Complete tables of bond distances, bond angles, and anisotropic thermal parameters for 2 and 3 (6 pages). Ordering information is given on any current masthead page.

OM9206259

(13) Sheldrick, G. M. *SHELXTL, an integrated system for solving, refining and displaying crystal structures from diffraction data*, Revision 5, University of Göttingen, Germany.

(14) TEXSAN-TEXRAY, Structure Analysis Package, Molecular Structure Corporation, 1985.